Am J Physiol Regul Integr Comp Physiol 297: R1409–R1420, 2009.
First published August 26, 2009; doi:10.1152/ajpregu.91038.2008.

pH regulating transporters in neurons from various chemosensitive brainstem regions in neonatal rats

Anna E. Kersh,[1] Lynn K. Hartzler,[1] Kevin Havlin,[1] Brittany Belcastro Hubbell,[1] Vivian Nanagas,[1] Avash Kalra,[1] Jason Chua,[1] Ryan Whitesell,[1] Nick A. Ritucci,[1] Jay B. Dean,[2] and Robert W. Putnam[1]

[1]*Department of Neuroscience, Cell Biology and Physiology, Wright State University Boonshoft School of Medicine, Dayton, Ohio; and* [2]*Department of Molecular Pharmacology and Physiology, College of Medicine, University of South Florida, Tampa, Florida*

Submitted 22 December 2008; accepted in final form 19 August 2009

Kersh AE, Hartzler LK, Havlin K, Belcastro Hubbell B, Nanagas V, Kalra A, Chua J, Whitesell R, Ritucci NA, Dean JB, Putnam RW. pH regulating transporters in neurons from various chemosensitive brainstem regions in neonatal rats. *Am J Physiol Regul Integr Comp Physiol* 297: R1409–R1420, 2009. First published August 26, 2009; doi:10.1152/ajpregu.91038.2008.—We studied the membrane transporters that mediate intracellular pH (pH_i) recovery from acidification in brainstem neurons from chemosensitive regions of neonatal rats. Individual neurons within brainstem slices from the retrotrapezoid nucleus (RTN), the nucleus tractus solitarii (NTS), and the locus coeruleus (LC) were studied using a pH-sensitive fluorescent dye and fluorescence imaging microscopy. The rate of pH_i recovery from an NH_4Cl-induced acidification was measured, and the effects of inhibitors of various pH-regulating transporters determined. Hypercapnia (15% CO_2) resulted in a maintained acidification in neurons from all three regions. Recovery in RTN neurons was nearly entirely eliminated by amiloride, an inhibitor of Na^+/H^+ exchange (NHE). Recovery in RTN neurons was blocked ~50% by inhibitors of isoform 1 of NHE (NHE-1) but very little by an inhibitor of NHE-3 or by DIDS (an inhibitor of HCO_3-dependent transport). In NTS neurons, amiloride blocked over 80% of the recovery, which was also blocked ~65% by inhibitors of NHE-1 and 26% blocked by an inhibitor of NHE-3. Recovery in LC neurons, in contrast, was unaffected by amiloride or blockers of NHE isoforms but was dependent on Na^+ and increased by external HCO_3^-. On the basis of these findings, pH_i recovery from acidification appears to be largely mediated by NHE-1 in RTN neurons, by NHE-1 and NHE-3 in NTS neurons, and by a Na- and HCO_3-dependent transporter in LC neurons. Thus, pH_i recovery is mediated by different pH-regulating transporters in neurons from different chemosensitive regions, but recovery is suppressed by hypercapnia in all of the neurons.

hypercapnia; locus coeruleus; Na^+/H^+ exchange; HCO_3 transport; NTS; retrotrapezoid nucleus

THE RESPONSE TO HYPERCAPNIA of brainstem neurons located in various chemosensitive regions is of major interest in the study of the control of respiration. Chemosensitive neurons have been defined as neurons that respond to changes of CO_2/H^+ and that are found in brainstem areas shown to alter ventilation when exposed to focal acidification (38). A maintained fall of intracellular pH (pH_i), with no pH_i recovery, has been shown to be an important component of the signaling pathway of hypercapnia in neurons from chemosensitive brainstem areas (17, 19, 38, 42, 51). However, these neurons do exhibit pH_i recovery from acidification when external pH is held constant (17, 19, 42). This recovery can be mediated by several different membrane transport proteins including Na^+/H^+ exchangers (NHE) (33), Na-driven Cl^-/HCO_3^- exchangers (NDCBE), and Na^+-HCO_3^- cotransporters (NBC-both electrogenic and electroneutral) (12, 37, 45). To our knowledge, there is no evidence for any functional HCO_3-dependent transporter in neurons from any central chemosensitive region.

Previous studies have suggested that NHE is the predominant transport protein mediating pH_i recovery from acidification in brainstem neurons (32, 42, 53). Under conditions of extracellular acidification, as with hypercapnic acidosis, NHE is inhibited and chemosensitive neurons do not exhibit pH_i recovery from acidification (41, 42). Several isoforms of the NHE protein exist and are found to be active in different parts of the body. Of the nine isoforms, only five are thought to be present in rat brains (12). NHE-1 is the ubiquitous isoform, is very sensitive to amiloride inhibition (37), and is completely inhibited by cariporide (HOE642). NHE-2 and NHE-3 are found predominantly in the gastrointestinal tract (3) and the kidney (37) but are also present in the brain. NHE-3 has a relatively specific inhibitor, S1611 (53, 58). The isoform NHE-4 is found in the hippocampus (7) and is thus not of interest in this study. NHE-5 is found in several regions of the rat brain, is closely related to NHE-3, and has no specific inhibitor (2).

Knowing that there are several isoforms of NHE present in the brain, the next issue to address is the question of which isoform is mediating pH_i recovery in neurons from various chemosensitive brainstem regions. We have evidence that amiloride inhibits recovery from acidification in neurons from the nucleus of the solitary tract (NTS) and the ventrolateral medulla (VLM) (42). Studies have also been conducted in the VLM showing that NHE-3 mediates pH_i regulation as well. Expression of mRNA for NHE-3 was found in some areas of the brain involved in respiratory control (23). When looking at cultured VLM neurons, exposure to NHE-3-specific inhibitors resulted in neuronal acidification and increased firing rate (58). In in vivo studies, specific NHE-3 inhibitors have been shown to stimulate the central respiratory system (22), and studies in which the brain-permeant NHE-3 inhibitor S8218 was applied to live rabbits showed that the drug caused an increase in ventilation (23). These studies suggest that NHE-3 is important in pH_i regulation in neurons from chemosensitive brainstem regions.

The aim of our study was to determine which pH-regulating transporters mediate recovery from acidification in neurons from three chemosensitive regions of the brainstem: the retrotrapezoid nucleus (RTN), the NTS, and the locus coeruleus

Address for reprint requests and other correspondence: R. W. Putnam, Dept. of Neuroscience, Cell Biology and Physiology, Wright State Univ. Boonshoft School of Medicine, Dayton, OH 45435 (e-mail: robert.putnam@wright.edu).

(LC). We particularly wanted to find evidence for any functional HCO_3-dependent transporters and which isoforms of NHE are active in the neurons from the various regions. We found that NHE-1 predominates in NTS and RTN neurons, with a smaller possible contribution from NHE-3, while a Na- and HCO_3-dependent transporter predominates in LC neurons.

A preliminary report of these data has been made (21).

MATERIALS AND METHODS

Solutions and materials. The normal solution, an artificial cerebrospinal fluid (aCSF), contained (in mM) 124 NaCl, 5 KCl, 2.4 $CaCl_2$, 1.3 $MgSO_4$, 1.24 KH_2PO_4, 26 $NaHCO_3$, and 10 glucose, and was equilibrated with 5% CO_2/balance O_2 (solution pH, pH_o, 7.45 at 37°C). NH_4Cl solutions of concentrations 40 and 75 mM were used for prepulse experiments [similar to previous values used in slices (42, 43)]. These solutions were prepared by substituting 40 mM or 75 mM NaCl with the equivalent concentration of NH_4Cl when preparing the aCSF solution. A 0 Na^+ aCSF solution was prepared by isosmotically replacing all sodium with *N*-methyl-D-glucamine (NMDG). Solution was continuously bubbled with 5% CO_2, and NMDG powder was added to reach a pH of 7.45 at 37°C. HEPES-buffered saline was identical to aCSF except that Na-HEPES replaced $NaHCO_3$ isosmotically, and the solution was equilibrated with 100% O_2 (41).

DIDS was purchased from Sigma (St. Louis, MO), and a 250-mM stock was prepared with DMSO-vehicle (had no effect on pH_i) and diluted to a final concentration of 500 μM. Amiloride was generously supplied by Merck, Sharp, and Dohme (Rahway, NJ), and a 0.5 M stock (made with DMSO) was diluted to a final concentration of 1–2 mM. The IC_{50} values of amiloride for NHE1 is 1–10 μM and for NHE3 is 100–400 μM, so amiloride should inhibit all NHE isoforms (25, 46). Stock solutions (5 mM concentration) were prepared in DMSO for cariporide (HOE642) and for S1611. The cariporide and S1611 IC_{50} values for NHE1 are 0.08 and 4.7 μM, respectively, and for NHE3 are 600–1,000 and 0.69 μM, respectively (25, 46). The stock solutions were diluted to 1 μM and 5 μM concentrations for each of the drugs, which were generously supplied to us by Sanofi-Aventis Pharmaceutical (Frankfurt am Main, Germany). Therefore, cariporide should offer a reasonable differentiation of NHE1 from NHE3 activity and, if anything, S1611 inhibition could be an overestimate of NHE3 activity (46). EIPA was made into a 200-mM stock with DMSO and was diluted to a final concentration of either 100 or 500 μM. The IC_{50} values of EIPA for NHE1 and NHE3 were 0.01–0.02 and 2–3 μM, respectively (25). The drug was purchased from Sigma. The pH_i calibration solution contained (in mM) 104 KCl, 1.24 KH_2PO_4, 1.3 $MgSO_4$, 2.4 $CaCl_2$, 25 NMDG-HEPES, 25 K-HEPES, 10 glucose, and 0.016 nigericin titrated with either KOH or HCl to reach a pH of 7.2. Nigericin was purchased from Sigma. A membrane-permeable acetoxymethyl ester form of [2′,7′-bis(2-carboxyethyl)-5-(and 6)-carboxyfluorescein] (BCECF), BCECF-AM (Invitrogen/Molecular Probes, Eugene, OR), was diluted with DMSO to a concentration of 20 μM.

Preparation of brain slices. All procedures involving animals were reviewed and approved by the Wright State University Animal Care and Use Committee and are in agreement with its guidelines (AALAC no. A3632–01). The techniques for slice preparation, BCECF dye loading, and imaging of BCECF-loaded slices have been previously described (17, 42, 43, 44). Briefly, brain slices were obtained from neonatal (P3 to P15) Sprague-Dawley rats of both sexes. Rats were killed by decapitation after cold anesthesia. The brainstem was removed and then sliced (300- to 400-μm thick) using a vibratome (model 101, series 1000; Pelco, St. Louis, MO). The vibratome was adjusted to slice at a speed of ~5 min per slice. Slices were cut into cold (5°C) aCSF equilibrated with 5% CO_2-95% O_2.

Identification of different brainstem regions. Slices were taken from three different brainstem regions (Fig. 1). To study the LC, pontine slices were cut rostrally for 1–1.5 mm from the level of the seventh cranial nerve (red lines and top slice in Fig. 1) (17). To study the RTN, slices were cut from the most caudal region of the facial nucleus for 600–900 μm rostrally (blue line and middle slice in Fig. 1) (44). To study the NTS, slices were cut up to 1.5 mm rostral from obex (green lines and bottom slice in Fig. 1) (42, 43). Neurons were studied from the regions indicated by the appropriate colors in the slices to the right in Fig. 1.

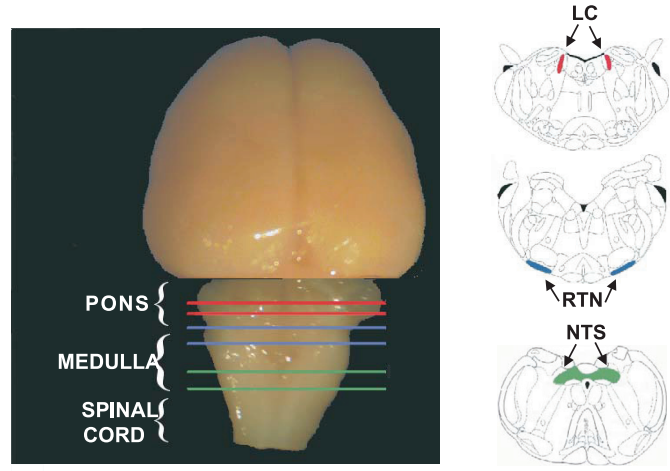

Fig. 1. Photograph of a dissected rat brain dorsal side up. The cerebellum has been removed so that the brainstem and proximal spinal cord are visible. Red lines delineate the area in the pons from which slices were taken to study the locus coeruleus (LC). Blue lines define the area spanning the pons and medulla from which the slices containing retrotrapezoid nucleus (RTN) were taken. Green lines show the area in the medulla from which slices were made to study the nucleus tractus solitarii (NTS). *Right*: drawings of representative transverse slices indicating the location of the LC (*top*), RTN (*middle*), and NTS (*bottom*).

BCECF dye-loading of slices. Slices were allowed to recover from slice trauma for at least 1 h in aCSF (room temperature) equilibrated with 5% CO_2-95% O_2. Slices were then transferred to a solution of aCSF containing 20 μM of the membrane-permeable form of BCECF and BCECF-AM and were incubated at 37°C for 30 min in the dark. Slices were then washed in dye-free aCSF solution at room temperature (equilibrated with 5% CO_2) until being used for experiments.

Imaging BCECF-loaded slices. BCECF fluorescence in slices was studied using a technique modified from Ritucci et al. (43). Briefly, a 75-W xenon arc lamp was used with a Lambda 10–2 filter wheel (Sutter Instruments, Austin, TX) to excite the slices alternately at 500 and 440 nm (filters from Omega Optical, Brattleboro, VT). Emitted fluorescence was collected at 530 nm and sent to a GenIIsys image intensifier and a charge-coupled device camera(model CCD72) (both from Dage-MTI, Michigan City, IN). The intensifier augmented the fluorescence images, which were then acquired by a Gateway 2000 486/25C computer. Images were collected and processed using Metafluor software (Molecular Devices, Downingtown, PA), which also was used to control the filter wheel. Images acquired at 500 nm and 440 nm excitation were divided to obtain a fluorescence ratio (R_{fl}), calculated as Fl_{500}/Fl_{440}. All images were displayed on a Sony RGB Trinitron superfine pitch monitor. By using the Define Graph Regions option in the MetaFluor software, individual neurons were selected from the R_{fl} image for analysis. Dye-loaded slices were exposed to a high-K^+/nigericin calibration solution (49) whose pH was 7.2, and a stable $R_{fl\text{-}calib}$ was obtained. All R_{fl} values were normalized to this value for a given neuron ($N_{fl} = R_{fl}/R_{fl\text{-}calib}$) and N_{fl} values were converted to pH_i values using the equation of Ritucci et al. (42) for NTS neurons, Filosa et al. (17) for LC neurons and Ritucci et al. (44) for RTN neurons. In all experiments the change in Fl_{440}, the excitation wavelength at which fluorescence is pH independent and

based solely on the amount of dye in the neuron, was monitored over time to assess cell viability. The data from a neuron was only used if its Fl_{440} value fell by $< 1\%$/min (6).

Experimental protocol. In a typical experiment, BCECF-loaded slices were placed on the stage of an inverted Nikon Diaphot microscope. The microscope was positioned on a Micro-g air table (Technical Manufacturing, Peabody, MA) to minimize vibrations during experiments. Slices were immobilized by the use of grids made of nylon fibers attached to a U-shaped stainless steel bar. Slices were continuously perfused with aCSF at 3–4 ml/min by using a gravity-feed system. All experiments were performed at 37°C. Upon commencement of the experiment, images were acquired, and the aCSF solution was superfused to wash cells until R_{fl} stabilized. Images were collected every 30–60 s throughout all experiments. In between measurements, the excitation light was blocked to prevent photobleaching of dye and photolytic damage to cells. Some neurons were acidified by exposure to hypercapnic acidotic solution (aCSF equilibrated with 15% CO_2, pH_o ~7.00). Most neurons were acidified using the NH_4Cl prepulse technique (8) with NH_4Cl exposures lasting for 15 ± 5 min (NH_4Cl exposure time and concentrations were varied in an attempt to obtain the same minimum pH_i with experimental solutions as seen with control exposures). Neurons acidified upon exposure to hypercapnic solutions and upon removal of the NH_4Cl, and recovery from these acidifications were quantified by determining the slopes of the pH_i vs. time traces. Neurons were allowed to recover until R_{fl} values reached a plateau. To determine the effects of various treatments on pH_i recovery rates, the exposure to aCSF containing the appropriate inhibitor was initiated upon removal of NH_4Cl. After the neuronal pH acidified and a recovery slope was clear, the neurons were then exposed to aCSF without the inhibitor, and recovery was followed until a plateau pH_i value was reached.

Data analysis and statistics. All values are reported as means ± 1 SE. The initial, maximum, minimum, and final pH values for each neuron were calculated by averaging 4–7 contiguous pH_i values at the appropriate part of the trace. All pH_i recovery slopes were estimated by least-squares regression lines fit to at least 10 points. In control experiments, least-squares regression lines were fitted from the point of minimum pH to the initial point of the pH plateau. In experimental trials, two recovery slopes were calculated. The first slope, representing the recovery of neurons exposed to the inhibitor or experimental drug, was fitted from the point of minimum pH_i to the last point of the exposure to the experimental solution. The second slope, representing recovery after cells were exposed to an inhibitor (when cells were returned to aCSF solution), was fitted from a point ~2 min after the return to normal solution to the initial point of the plateau.

All comparisons of three or more means were done with a one-way ANOVA. Multiple paired comparisons were performed using a Tukey-Kramer test. The level of significance was $P < 0.05$.

RESULTS

Initial values of pH_i. We determined the initial value for pH_i in aCSF equilibrated with 5% CO_2 for neurons from three brainstem regions. Initial pH_i varied and was 7.31 ± 0.003 ($n = 304$), 7.43 ± 0.005 ($n = 266$), and 7.34 ± 0.001 ($n = 349$) for RTN, NTS, and LC neurons, respectively. These values are somewhat more alkaline than pH_i values reported for neurons from another chemosensitive region, the medullary raphé (9). Differences in pH_i values measured in neurons from different regions have been discussed previously (43). The lower pH_i values in raphé neurons may reflect the fact that these neurons were studied in cell culture, which has been shown previously to reduce the measured value of pH_i (39). Statistical analysis (1-way ANOVA with Tukey-Kramer pairwise tests) showed that NTS neurons were significantly ($P < 0.001$) more alkaline than RTN and LC neurons, as has previously been observed (17, 42, 43, 44), and the small difference in pH_i between RTN and LC neurons was also significantly different ($P < 0.001$).

pH_i response to hypercapnia. We measured the pH_i response to hypercapnia in neurons from the RTN, NTS, and LC. Neurons from the RTN had an initial pH_i of 7.29 ± 0.001 and acidified in response to hypercapnia (15% CO_2) to a minimum pH_i of 7.09 ± 0.007 ($n = 25$) (Fig. 2*A*). RTN neurons did not recover from hypercapnia-induced acidification (−0.0017 ± 0.0007 pH_i/min) ($n = 25$) (Fig. 2, *A* and *D*, white bar). Upon return to normocapnic (5% CO_2) aCSF, pH_i returned toward its original value (7.17 ± 0.036) ($n = 25$) (Fig. 2*A*). In response to hypercapnia, neurons from the NTS acidified to a minimum pH_i of 7.22 ± 0.007 from an initial pH_i of 7.41 ± 0.009 ($n = 24$) (Fig. 2*B*) and showed no recovery from acidification (−0.0008 ± 0.0010 pH_i/min) ($n = 24$) (Fig. 2, *B* and *D*, white bar). After CO_2 levels were returned to normal, NTS neuron pH_i returned to 7.41 ± 0.010 ($n = 24$) (Fig. 2*B*). Neurons from the LC had an initial pH_i of 7.34 ± 0.002 and acidified in response to hypercapnia to a minimum pH_i of 7.17 ± 0.004 ($n = 74$) (Fig. 2*C*). LC neurons did not recover from hypercapnia-induced acidification (−0.0030 ± 0.0004 pH_i/min) ($n = 24$) (Fig. 2, *C* and *D*, white bar). After CO_2 levels were returned to normal, LC neuron pH_i returned to normal (7.34 ± 0.003) ($n = 24$) (Fig. 2*C*). Thus, neurons from all three regions acidified in response to hypercapnia, and this acidification was maintained in the maintained presence of hypercapnia.

The NH_4Cl prepulse. The purpose of these experiments was to determine which transport protein regulates pH_i recovery from acidification in the neurons from three chemosensitive brainstem regions: the RTN, NTS, and LC. In all experiments, cells were exposed to an NH_4Cl prepulse. Experiments in the RTN began with cells having an initial pH of 7.29 ± 0.002 ($n = 26$). Once the NH_4Cl was removed, RTN neurons acidified to a minimum pH of 7.04 ± 0.010 ($n = 26$). RTN cells recovered from this acidification (in the presence of aCSF) at a rate of 0.0138 ± 0.0004 pH_i/min ($n = 26$) (Fig. 2*D*, black bar; Fig. 3*A*, black line; Fig. 3*B*, black bar). Cells in the NTS had an initial pH_i value of 7.42 ± 0.017 and acidified after the NH_4Cl prepulse to a minimum pH_i of 7.19 ± 0.011 ($n = 46$). Recovery (in the presence of aCSF) proceeded at a rate of 0.0156 ± 0.0008 pH_i/min ($n = 46$) (see Fig. 2*D*, black bar; Fig. 4*A*, black line; Fig. 4*B*, black bar). LC neurons acidified from an initial pH_i value of 7.34 ± 0.0006 to a minimum pH_i of 7.15 ± 0.0058 ($n = 52$). Recovery occurred but at a significantly ($P < 0.001$) slower rate of 0.0090 ± 0.0005 pH_i/min ($n = 52$) (Fig. 2*D*, black bar; Fig. 5*A*, black line; Fig. 5*B*, black bar). These data clearly show that the lack of pH_i recovery from hypercapnia-induced acidification is not due to the lack of pH-regulating transporters, since neurons from all three brainstem regions exhibited pH_i recovery from acidification induced by an NH_4Cl prepulse.

General transport inhibitors. To study the transmembrane transport systems that mediate pH_i recovery in these neurons, we used both general and specific inhibitors of pH-regulating transporters. These pH-regulating transporters most likely include one or more isoforms of the NHE and one or more of several HCO_3-dependent exchangers (37). Tests were conducted to determine what type of exchange protein mediates pH_i recovery in neurons from the RTN, NTS, and LC.

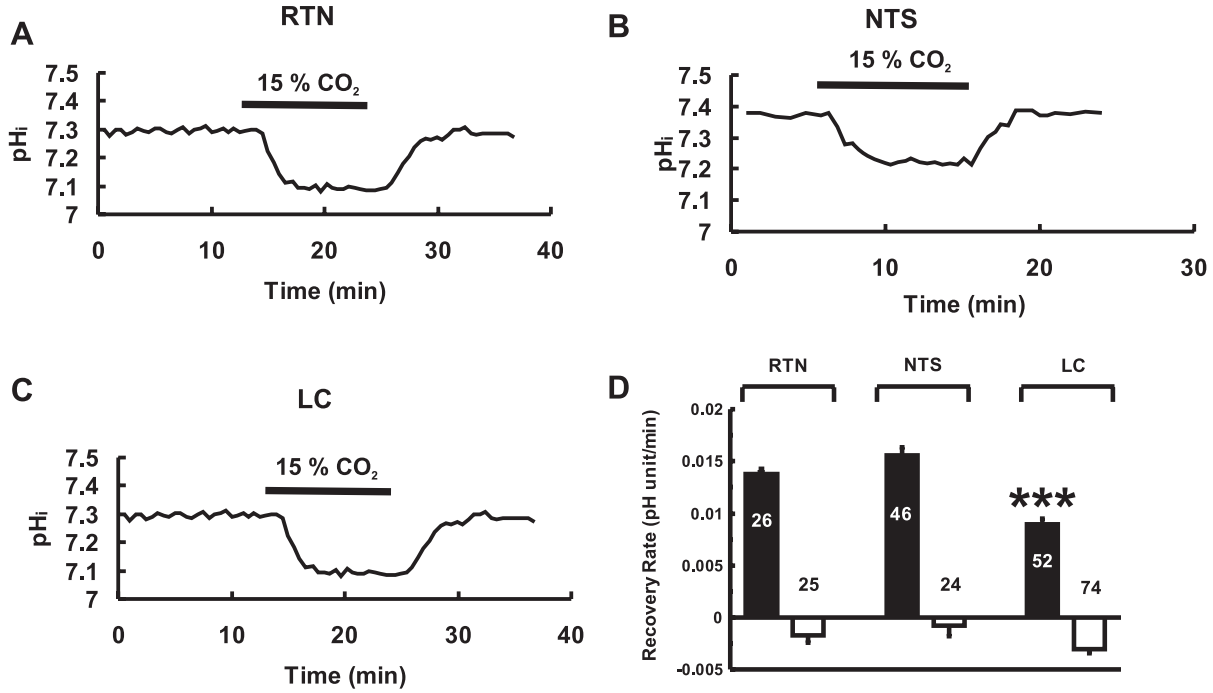

Fig. 2. Effect of hypercapnia (15% CO_2) on pH_i in RTN, NTS, and LC neurons. Hypercapnia results in a maintained acidification with no pH_i recovery in RTN neuron (*A*) NTS neuron (*B*), or LC neuron (*C*). *D*: summary of the pH_i recovery from NH_4Cl-induced acidification (black bars) or during hypercapnia (white bars) in RTN, NTS, and LC neurons. The height of a bar represents the mean recovery rate (pH U/min) ± 1 SE. The number in or above each bar represents the number of neurons. ***Recovery from NH_4Cl-induced acidification is significantly different in LC neurons than the recovery in RTN and NTS neurons at $P < 0.001$.

Na^+-free solution. Cells from all three regions were exposed to Na^+-free aCSF to see if the pH_i recovery from NH_4Cl-induced acidification was Na^+ dependent. The recovery rate of RTN neurons for the duration of the exposure to Na^+-free solution was 0.0030 ± 0.0012 pH_i/min ($n = 10$) (Fig. 3*A*, red line, Fig. 3*B*, red bar). This represents an 86% reduction compared with the recovery upon readdition of Na^+ ($P < 0.001$), which amounted to 0.0212 ± 0.0017 pH_i/min ($n = 10$) (Fig. 3*A*, red line). Similar results were found for neurons from the other two regions. When NTS neurons were acidified, recovery rate in Na^+-free solution was 0.0050 ± 0.0022 pH_i/min ($n = 12$) (Fig. 4*A*, red line, Fig. 4*B*, red bar) and increased to a rate of 0.0259 ± 0.0043 pH_i/min ($n = 12$) upon readdition of Na^+ (Fig. 4*A*, red line). Thus, Na^+ free solutions inhibited recovery in NTS neurons by 81% compared with recovery upon readdition of Na^+ ($P < 0.001$). LC neurons showed recovery at a rate of −0.0033 ± 0.0004 pH_i/min ($n = 34$) in Na^+-free solution (Fig. 5*A*, red line; Fig. 5*B*, red bar). The recovery rate increased to 0.0259 ± 0.0062 pH_i/min ($n = 34$) upon readdition of Na^+ (Fig. 5*A*, red line). Therefore, pH_i recovery from acidification in LC neurons was completely inhibited in Na^+-free solutions. These data show that pH_i recovery from acidification is largely Na^+-dependent in neurons from all three brainstem regions. It is evident that NH_4Cl results in a larger acidification in the presence of Na^+-free solutions. This common observation is due to a larger acidification upon inhibition of pH-recovery mechanisms and the possible reversal of alkalinizing recovery systems, resulting in acidification of pH_i. This greater acidification in Na^+-free solutions should result in greater pH_i recovery so the inhibition of recovery by Na^+-free solutions is even more striking. Thus, the greater NH_4Cl-induced acidification seen in Na^+-free solutions is further confirmation of the importance of Na^+-dependent transporters in neurons from the RTN, NTS, and LC.

Amiloride. We next tested the ability of amiloride (1 mM), a known inhibitor of NHE, to inhibit pH_i recovery in brainstem neurons. In RTN neurons, recovery rate was 0.0010 ± 0.0007 pH_i/min ($n = 25$) (Fig. 3*A*, dark blue line; Fig. 3*B*, dark blue bar) in the presence of amiloride (1 mM) and increased to 0.0152 ± 0.0018 pH_i/min ($n = 25$) upon removal of amiloride, indicating that amiloride inhibited recovery in RTN neurons by 93%. Similarly, amiloride inhibited recovery in NTS neurons, which had a recovery rate of 0.0063 ± 0.0006 pH_i/min ($n = 42$) (Fig. 4*A*, dark blue line; Fig. 4*B*, dark blue bar) in the presence of amiloride and 0.0140 ± 0.0011 pH_i/min ($n = 42$) after its removal, amounting to a 65% inhibition. In contrast, amiloride not only did not inhibit but increased recovery in LC neurons, which had a recovery rate of 0.0157 ± 0.0007 pH_i/min ($n = 32$) (Fig. 5*A*, dark blue line; Fig. 5*B*, dark blue bar) in the presence of amiloride and 0.0107 ± 0.0034 pH_i/min ($n = 32$) after its removal (Fig. 5*A*, dark blue line). The increased recovery may be due to the fact that amiloride caused a larger NH_4Cl-induced acidification (minimum pH_i of 7.00 in the presence of amiloride vs. 7.15 in its absence), which should increase recovery rate. We do not know why amiloride enhances the cell acidification induced by the NH_4Cl prepulse. In summary, pH_i recovery was largely inhibited by amiloride in RTN and NTS neurons but not inhibited by amiloride in LC neurons.

DIDS. Cells from all regions were exposed to DIDS, an inhibitor of HCO_3-dependent transporters (37). In RTN neurons, recovery rate was 0.0156 ± 0.0018 pH_i/min ($n = 10$)

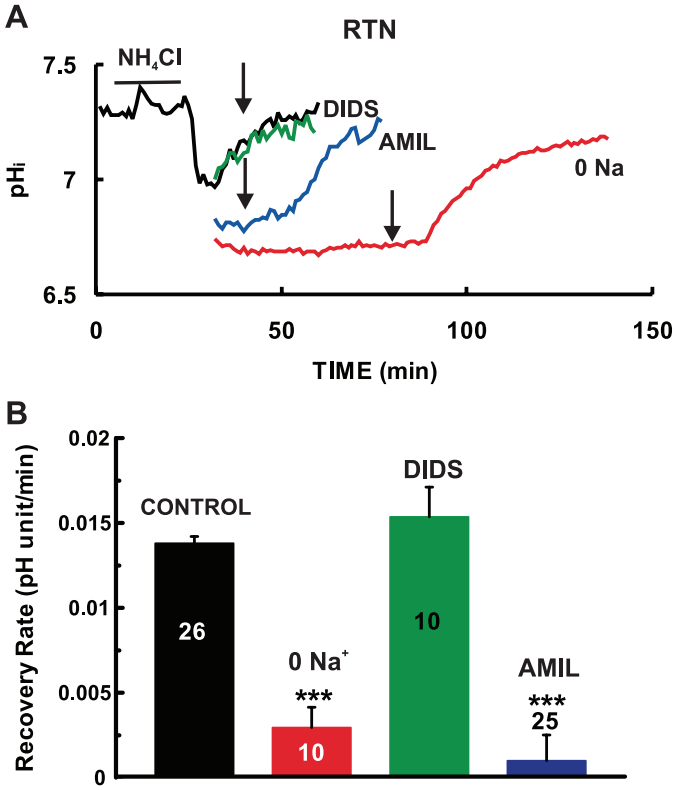

Fig. 3. Effect of various drugs and ion substitution on pH_i recovery from an NH_4Cl prepulse-induced acidification in RTN neurons. *A*: black line shows the pH_i response of an RTN neuron to an NH_4Cl prepulse (40 mM), including a control pH_i recovery in the presence of artificial cerebrospinal fluid (aCSF). Colored lines show the recovery of cells in the presence of 0.5 mM DIDS (green), 1 mM amiloride (AMIL; blue), and 0 Na^+ aCSF [*N*-methyl-D-glucamine (NMDG) substitution; red]. Arrows indicate the time at which the experimental solutions were replaced with aCSF. *B*: summary of pH_i recovery in RTN neurons under various conditions. Height of bars represent the mean recovery rate (pH U/min) ± 1 SE. Number (in or above each bar) = number of neurons. ***Recovery is significantly different than control recovery at $P < 0.001$.

(Fig. 3*A*, dark green line; Fig. 3*B* dark green bar) in the presence of DIDS (0.5 mM) and was 0.0102 ± 0.0015 pH_i/min ($n = 10$) upon removal of DIDS (Fig. 3*A*, dark green line), indicating that DIDS did not inhibit recovery in RTN neurons. Similarly, DIDS did not inhibit recovery in NTS neurons, which had a recovery rate of 0.0115 ± 0.0014 pH_i/min ($n = 12$) (Fig. 4*A*, dark green line; Fig. 4*B*, dark green bar) in the presence of DIDS and 0.0116 ± 0.0010 pH_i/min ($n = 12$) after its removal (Fig. 4*A*, dark green line). DIDS also did not inhibit recovery in LC neurons, which had a recovery rate of 0.0090 ± 0.0007 pH_i/min ($n = 17$) (Fig. 5*A*, dark green line; Fig. 5*B*, dark green bar) in the presence of DIDS and 0.0090 ± 0.0005 pH_i/min ($n = 17$) after its removal (Fig. 5*A*, dark green line). The lack of an effect of DIDS on recovery in neurons from all three regions suggests that DIDS-inhibitable HCO_3-dependent transporters do not play a significant role in pH_i recovery from acidification in RTN, NTS, and LC neurons.

NHE isoform inhibitors. Our findings imply that NHE appears to be the predominant pH-regulating transporter mediating recovery from cell acidification, at least in RTN and NTS neurons. This raises the question of which isoform of NHE is active in pH_i regulation in neurons from these brainstem regions. Three main isoforms of NHE are present in the rat brain: NHE-1, NHE-3, and NHE-5 (2, 24, 56, 58), although there is some evidence for NHE-2 and NHE-4 expression in brainstem (24). Specific inhibitors are available for NHE-1 (25) and NHE-3 (23, 46, 58); thus our study focused on these isoforms.

EIPA. EIPA is an amiloride derivative and an inhibitor of NHE, which is slightly more specific for the NHE-1 isoform (25). The effects of both 0.1 and 0.5 mM EIPA on the recovery from acidification were determined. Since the effects of EIPA were found not to be reversible, the inhibition of recovery was calculated using control recovery values (see *The NH_4Cl prepulse*). EIPA reduced recovery in RTN neurons to 0.0072 ± 0.0011 pH_i/min ($n = 8$) and to 0.0048 ± 0.0008 pH_i/min ($n = 11$) for 0.1 and 0.5 mM (Fig. 6*A*, yellow line; Fig. 6*B*, yellow bar), respectively. This amounts to 48 and 65% inhibition of recovery. For NTS neurons, recovery was reduced by EIPA to 0.0078 ± 0.0008 pH_i/min ($n = 48$) and 0.0090 ± 0.0060 pH_i/min ($n = 25$) (Fig. 7*A*, yellow line; Fig. 7*B*, yellow bar). This amounts to 50 and 42% inhibition of recovery. Finally, recovery of LC neurons in 0.1 mM EIPA was 0.010 ± 0.0008 pH_i/min ($n = 26$) and in 0.5 mM EIPA was 0.0060 ± 0.0011 pH_i/min ($n = 23$) (Fig. 8*A*, yellow line; Fig. 8*B*, yellow bar), amounting to 0 and 33% inhibition. These findings suggest that NHE-1 may account for about half of the recovery in RTN and NTS neurons, but a smaller fraction in LC neurons.

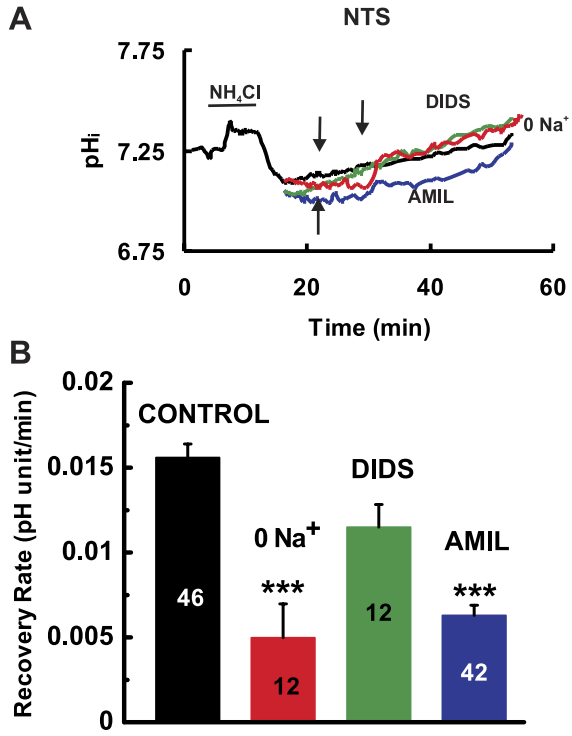

Fig. 4. Effect of various drugs and ion substitution on pH_i recovery from an NH_4Cl prepulse-induced acidification in NTS neurons. *A*: black line shows the pH_i response of an NTS neuron to an NH_4Cl prepulse (40 mM), including a control pH_i recovery in the presence of aCSF. Colored lines show the recovery of cells in the presence of 0.5 mM DIDS (green), 1 mM AMIL (blue), and 0 Na^+ aCSF (NMDG substitution; red). Arrows indicate the time at which the experimental solutions were replaced with aCSF. *B*: summary of pH_i recovery in NTS neurons under various conditions. Height of bars represent the mean recovery rate (pH U/min) ± 1 SE. Number in each bar = number of neurons. ***Recovery is significantly different than control recovery at $P < 0.001$.

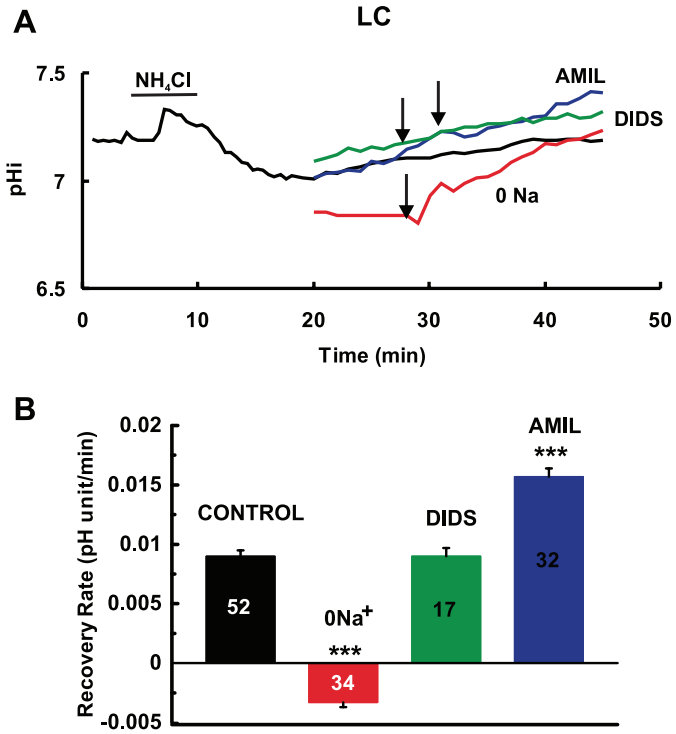

Fig. 5. Effect of various drugs and ion substitution on pH_i recovery from an NH_4Cl prepulse-induced acidification in LC neurons. *A*: black line shows the pH_i response of an LC neuron to an NH_4Cl prepulse (40 mM), including a control pH_i recovery in the presence of aCSF. Colored lines show the recovery of cells in the presence of 0.5 mM DIDS (green), 1 mM AMIL (blue), and 0 Na^+ aCSF (NMDG substitution; red). Arrows indicate the times at which the experimental solutions were replaced with aCSF. *B*: summary of pH_i recovery in LC neurons under various conditions. Height of bars represent the mean recovery rate (pH U/min) ± 1 SE. Number in each bar = number of neurons. ***Recovery is significantly different than control recovery at $P < 0.001$.

Cariporide. Cariporide (HOE642) is a much more specific NHE-1 inhibitor than EIPA (25). Two concentrations of cariporide were tested in these experiments. At 1 μM, cariporide inhibited recovery only in NTS neurons, where recovery was 0.0075 ± 0.0006 pH_i/min ($n = 7$) (Fig. 7*B*, white bar) in the presence and 0.0154 ± 0.0013 pH_i/min ($n = 7$) in the absence of cariporide, an inhibition of 50%. At 5 μM, cariporide inhibited recovery in RTN and NTS neurons, but not in LC neurons. In RTN neurons, recovery was 0.0078 ± 0.0012 pH_i/min ($n = 58$) (Fig. 6*A*, light blue line; Fig. 6*B*, light blue bar) in the presence and 0.0131 ± 0.0008 pH_i/min ($n = 58$) (Fig. 6*A*, light blue line) upon removal of 5 μM cariporide, an inhibition of 40%. At 5 μM cariporide, recovery in NTS neurons was 0.0051 ± 0.0007 pH_i/min ($n = 27$) (Fig. 7*A*, light blue line; Fig. 7*B*, light blue bar), which increased to 0.0194 ± 0.0017 pH_i/min ($n = 27$) upon removal of cariporide (Fig. 7*A*, light blue line), amounting to an inhibition of recovery by 74%. Finally, 5 μM cariporide did not inhibit recovery in LC neurons, which was 0.0110 ± 0.0009 pH_i/min ($n = 42$) (Fig. 8*A*, light blue line; Fig. 8*B*, light blue bar) in the presence and 0.012 ± 0.0016 pH_i/min ($n = 42$) in the absence (Fig. 8*A*, light blue line) of cariporide. In general, the results with cariporide are similar to those with EIPA, with ~50% of the recovery inhibited in RTN and NTS neurons but very little in LC neurons.

S1611. S1611 is a reasonably specific inhibitor for NHE-3 (46). S1611 at 1 μM had no effect on pH_i recovery in neurons from any of the three brainstem areas. At 5 μM, S1611 also had no effect on the recovery from acidification in RTN neurons (rate of 0.0194 ± 0.0015 pH_i/min in the presence and 0.0181 ± 0.0019 pH_i/min in the absence of S1611, $n = 28$) (Fig. 6*A* light green line; Fig. 6*B*, light green bar) and in LC neurons (rate of 0.0090 ± 0.0005 pH_i/min in the presence and 0.0090 ± 0.0006 pH_i/min in the absence of S1611, $n = 44$) (Fig. 8*A*, light green line; Fig. 8*B*, light green bar). In NTS neurons, 5 μM S1611 caused an inhibition (26%) of pH_i recovery (rate of 0.0109 ± 0.0010 pH_i/min in the presence and 0.0147 ± 0.0007 pH_i/min in the absence of S1611, $n = 38$) (Fig. 7*A*, light green line; Fig. 7*B*, light green bar). Thus, we have some evidence that the NHE-3 isoform participates in pH_i recovery in NTS neurons.

The neurons from the RTN, NTS, and LC are heterogeneous in their properties (1, 26, 29), and thus it may be that a small pocket of neurons in each area express NHE-3. For instance, a small group of neurons has been suggested to be responsible

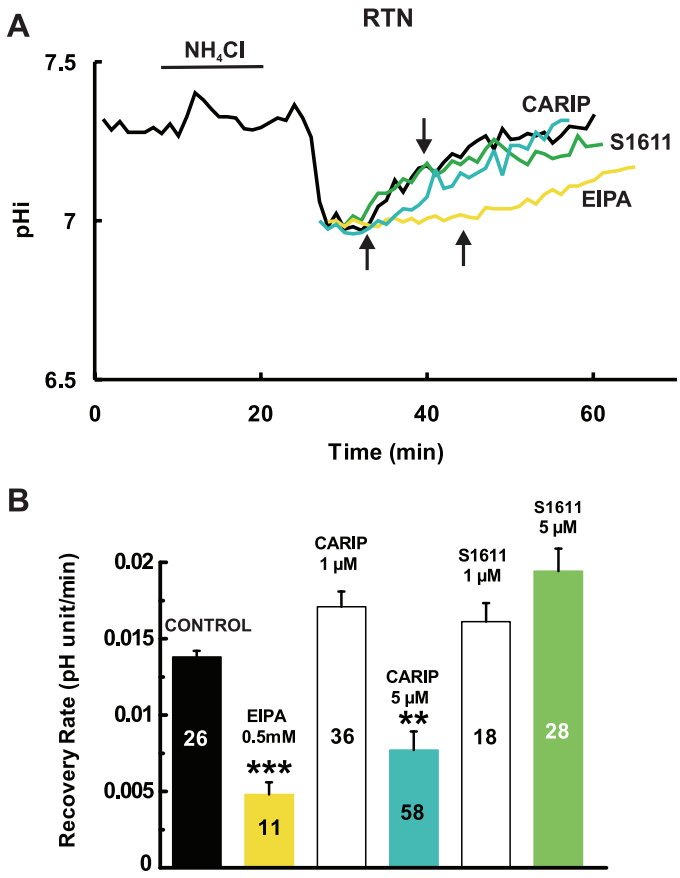

Fig. 6. Effect of the Na^+/H^+ exchange (NHE)-1 inhibitors (EIPA and cariporide) and an NHE-3 inhibitor (S1611) on pH_i recovery from an NH_4Cl prepulse-induced acidification in RTN neurons. *A*: black line shows the pH_i response of an RTN neuron to an NH_4Cl prepulse (40 mM), including a control pH_i recovery in the presence of aCSF. Colored lines show the pH_i recovery of cells in the presence of 0.5 mM EIPA (yellow), 5 μM cariporide (CARIP; light blue), or S1611 (light green). Arrows indicate time at which inhibitors were replaced by aCSF. *B*: summary of the effects of NHE inhibitors on pH_i recovery in RTN neurons. Height of bars represent mean recovery rate (pH U/min) ± 1 SE. Number in each bar = number of neurons. Recovery was significantly different than control recovery at $^{**}P < 0.01$ and $^{***}P < 0.001$.

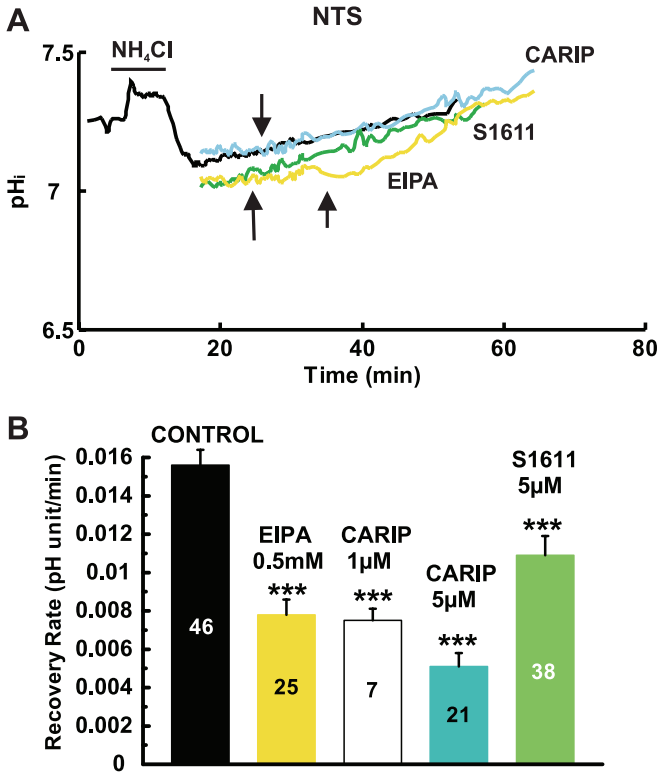

Fig. 7. Effect of the NHE-1 inhibitors (EIPA and cariporide) and an NHE-3 inhibitor (S1611) on pH_i recovery from an NH_4Cl prepulse-induced acidification in NTS neurons. *A*: black line shows the pH_i response of an NTS neuron to an NH_4Cl prepulse (40 mM), including a control pH_i recovery in the presence of aCSF. Colored lines show the pH_i recovery of cells in the presence of 0.5 mM EIPA (yellow), 5 μM cariporide (CARIP; light blue), or S1611 (light green). Arrows indicate time at which inhibitors were replaced by aCSF. *B*: summary of the effects of NHE inhibitors on pH_i recovery in NTS neurons. Height of bars represent mean recovery rate (pH U/min) ± 1 SE. Number in each bar = number of neurons. ***Recovery is significantly different than control recovery at $P < 0.001$.

for chemosensitivity in the RTN (26). To determine whether we have a small percentage of neurons containing NHE-3 in each area, we looked at the individual recovery of each neuron in the presence of 5 μM S1611. We used two criteria to define an inhibited neuron. The first criterion was that, if the recovery in the presence of S1611 was < 33% of the control recovery, then recovery in that neuron was judged to be inhibited by S1611. The second criteria was that, if the recovery in the presence of S1611 was less than the lowest recovery in control neurons, then that neuron was judged to have recovery inhibited by S1611. For RTN neurons, the control recovery rate averaged 0.0138 pH_i/min, and the range of recovery rates was 0.0110 to 0.0202 pH_i/min. Thus, a neuron was considered to be inhibited by S1611 if its recovery was < 0.0046 pH_i/min (*criterion 1*) or < 0.0110 pH_i/min (*criterion 2*). Only one out of 28 neurons (3.6%) met *criterion 1*, while three out of 28 (10.7%) met *criterion 2*. Thus, at most, 5–10% of RTN neurons might contain significant amounts of NHE-3. NTS neurons exhibited control recovery rates of 0.0156 pH_i/min with a range of 0.0054 to 0.0279 pH_i/min, so recovery needed to be < 0.0051 (*criterion 1*) or 0.0054 (*criterion 2*) pH_i/min in the presence of S1611 to be considered inhibited. For both criteria, seven out of 38 neurons (18.4%) appeared to contain NHE-3 activity. Finally, LC neurons had a control recovery rate of 0.009 pH_i/min with a range of 0.0043 to 0.0260 pH_i/min. Recovery needed to be < 0.003 (*criterion 1*) or 0.0043 (*criterion 2*) pH_i/min in the presence of S1611 to be considered inhibited. Only one out of 44 neurons (2.3%) met these criteria. Thus, at most, 2–3% of LC neurons appear to contain NHE-3.

HCO_3-dependent recovery in LC neurons. Our findings suggest that NHE does not play a major role in the pH_i recovery from acidification in LC neurons, yet no DIDS-inhibitable recovery was evident either. To see whether HCO_3-dependent transport could play a role in pH_i regulation in LC neurons, we studied recovery in the presence and in the nominal absence of HCO_3. In aCSF, LC neurons exhibited brisk recovery from an NH_4Cl prepulse-induced intracellular acidification (Fig. 9, *A* and *B*). Interestingly, the same experiment in HEPES-buffered medium showed a significantly slower pH_i recovery (Fig. 9, *A* and *B*), despite the fact that the total buffering power of these cells is much smaller, and thus the rate of pH_i recovery should be larger (37). We note that the recovery rate of these LC neurons in CO_2 is larger than reported earlier (compare control recovery in Fig. 5*B* with CO_2 recovery in Fig. 9*B*). The larger recovery in these experiments is most likely due to the greater NH_4Cl-induced acidification in the experiments in Fig. 9 (minimum pH_i ~6.65) compared with the experiments in Fig. 5 (minimum pH_i ~7.15). The findings of higher pH_i recovery in the presence vs. the absence

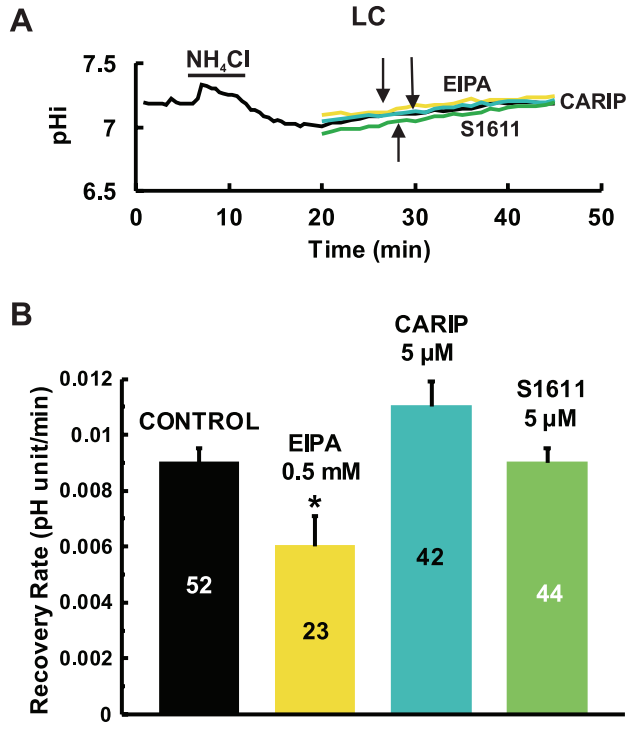

Fig. 8. Effect of the NHE-1 inhibitors (EIPA and cariporide) and an NHE-3 inhibitor (S1611) on pH_i recovery from an NH_4Cl prepulse-induced acidification in LC neurons. *A*: black line shows the pH_i response of an LC neuron to an NH_4Cl prepulse (40 mM), including a control pH_i recovery in the presence of aCSF. Colored lines show the pH_i recovery of cells in the presence of 0.5 mM EIPA (yellow), 5 μM cariporide (CARIP; light blue), or S1611 (light green). Arrows indicate times at which inhibitors were replaced by aCSF. *B*: summary of the effects of NHE inhibitors on pH_i recovery in LC neurons. Height of bars represent the mean recovery rate (pH U/min) ± 1 SE. Number in each bar = number of neurons. *Recovery is significantly different than control recovery at $P < 0.05$.

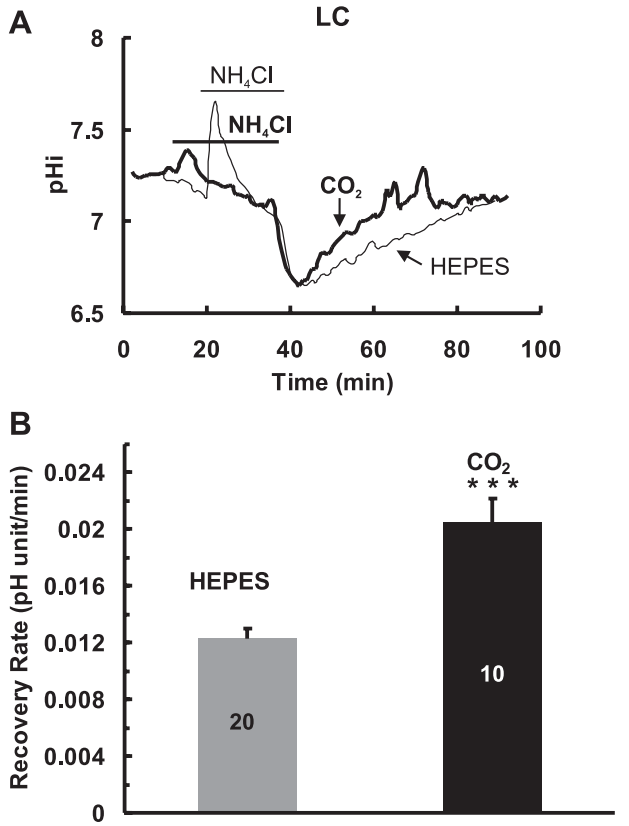

Fig. 9. Recovery of pH_i from NH_4Cl-induced (40 mM) acidification in the absence and presence of CO_2 in LC neurons. *A*: thin line shows the pH_i response to an NH_4Cl-induced (40 mM) acidification in HEPES-buffered medium (nominal absence of CO_2/HCO_3). Thick line shows the pH_i response to an NH_4Cl-induced acidification in CO_2/HCO_3-buffered medium (5% CO_2/26 mM HCO_3). Note that recovery is faster in CO_2/HCO_3-buffered medium, although total intracellular buffering power is higher in this medium. *B*: mean recovery from NH_4Cl-induced (40 mM) acidification in the presence (black bar) and absence (gray bar) of CO_2 in LC neurons. Height of bars represent the mean recovery rate (pH U/min) ± 1 SE. Number in each bar = number of neurons. ***Recovery is significantly different in CO_2- vs. HEPES-buffered medium at $P < 0.001$.

of CO_2 indicate that pH_i recovery from acidification in LC neurons is faster in the presence of HCO_3, suggesting that a HCO_3-dependent transporter is important for pH_i regulation in LC neurons.

DISCUSSION

There are several main conclusions from our data. First, in neurons from the neonatal brainstem, recovery from acidification appears to be largely mediated by Na-dependent processes. Second, NHEs account for nearly all recovery from intracellular acidification in RTN and NTS neurons, with NHE-1 appearing to be predominant. Third, NHE-3 is present in, at most, a small percentage of brainstem neurons, but may account for up to 10% of recovery in RTN neurons and 20% of recovery in NTS neurons. Finally, recovery from acidification in LC neurons appears to be mediated largely by a DIDS-insensitive and Na- and HCO_3-dependent transporter. Despite the presence of different pH-regulating transporters in the different brainstem regions, pH_i did not exhibit any recovery from hypercapnia-induced acidification in the neurons from all three regions.

Neuronal pH_i-regulating transporters. There are two main groups of pH-regulating transporters. One group is the SLC4 family of HCO_3-dependent transporters (45). The SLC4 family consists of a number of transporters including Cl^-/HCO_3^- exchangers (AE), which normally mediate HCO_3^- efflux in exchange for Cl^- influx, thus acidifying cells in response to alkalinization. The clearest evidence for functional HCO_3-dependent transport in neurons is for AE, its activity having been demonstrated in cultured neurons from the cerebellum (18), the hippocampus (39), and the cortex (34), as well as medullary neurons within brainstem slices, including neurons from chemosensitive regions (41). In response to an acid load, there are many HCO_3-dependent transporters that can contribute to alkalinizing pH_i recovery, including electrogenic NBCe, electroneutral NBCs (NBCn1 and NBCn2), and electroneutral NDCBE (45). NDCBE activity has been demonstrated in freshly dissociated hippocampal neurons from the CA1 region (4, 47) and cultured sympathetic (50) and cerebellar (36) neurons. While NBCe appears to be largely localized to glia (5), NBCn1 have been reported in rat hippocampal neurons (14) and, interestingly, it is largely insensitive to inhibition by DIDS (13). To date, however, no functional HCO_3-dependent transporter, other than AE, has been shown to be active in neurons from putative chemosensitive regions.

The other main group of pH-regulating transporters is the SLC9 gene family of NHE (33). In contrast to HCO_3-dependent transporters, NHE isoforms appear to play a major role in neuronal pH_i responses to acidification (37). Nine isoforms of NHE have been identified, but isoforms six through nine are found exclusively within the cell (27). Of the five remaining isoforms, NHE-1 is ubiquitous, with a high level of mRNA expression throughout the brain and brainstem (24), and functional NHE-1 is likely, at least in brainstem (41). This isoform is characterized by a high sensitivity to inhibition by amiloride, EIPA, and cariporide but a much lower sensitivity to S1611 (25, 46). NHE-2 mRNA has been detected at much lower levels than NHE-1 mRNA in the brain (24, 52), but the expression of the protein has been found to be low in the brain and brainstem (59), suggesting that the NHE-2 protein is not crucial to pH regulation in the brainstem. NHE-3 mRNA has been detected at very low levels in the brainstem but appears to be present at somewhat greater levels in the cerebellum (24). Functional NHE-3 has been suggested to be present in a few neurons from the VLM (53, 58). It is characterized by relatively low sensitivity to inhibition by amiloride and cariporide but higher sensitivity to inhibition by S1611 or related compounds (11, 25, 46). NHE-4 mRNA, but not protein, has been reported at low levels in the brain (24, 35), although some expression of NHE-4 has been found in hippocampal neurons (7). NHE-4 protein has not been detected in the brainstem. NHE-4 is highly resistant to inhibition by amiloride and EIPA (25) and is not activated by cell acidification (7). NHE-5 is unique among the NHEs because it is highly expressed in the rat brain, with little expression elsewhere (2). NHE-5 is structurally similar to NHE-3, and is similarly resistant to EIPA and amiloride but is not sensitive to S1611 (Dr. Klaus Wirth, Sanofi-Aventis Pharmaceutical, Frankfurt, Germany, personal communication).

In summary, since our study focuses on the mode of internal pH regulation in neurons from chemosensitive regions, we are mainly concerned with the NHE isoforms likely to be found in

neurons from these regions. Of the five NHE isoforms that reside in the cell membrane, NHE-1, 3, and 5 are most likely to be present in the brainstem. We are also interested in any evidence for functional HCO_3-dependent transport in neurons from putative chemosensitive brainstem regions.

pH-regulating transporters in RTN, NTS, and LC neurons. While we recognize the limitations of purely pharmacological studies, we believe that our data comparing the responses of pH_i recovery among neurons from different brainstem areas with multiple NHE inhibitors does offer an initial indication of the pattern of the presence of pH-regulating transporters in the neurons from the RTN, NTS, and LC. These patterns will ultimately have to be confirmed by molecular and immunocytochemical techniques.

In RTN neurons, recovery is nearly completely inhibited by Na-free solutions and by amiloride, but unaffected by DIDS (Table 1). These findings agree with earlier work on RTN neurons showing amiloride-sensitive pH_i recovery from acidification (32). Thus, the vast majority of recovery from acidification in RTN neurons appears to be mediated by NHE. Since EIPA and cariporide inhibit about half of this recovery, we assume that NHE-1 accounts for at least half of the pH_i recovery in RTN neurons. S1611 inhibits recovery in ~5–10% of these neurons, indicating, at most, a small presence of NHE-3 in RTN neurons. The remainder of recovery may possibly be due to NHE-5. These data indicate that recovery from acidification in RTN neurons is likely due to multiple NHE isoforms, with NHE-1 playing the predominant role.

Similarly, recovery from intracellular acidification in NTS neurons is largely inhibited by amiloride and Na-free solutions and unaffected by DIDS (Table 1), as previously reported (41, 42). Since EIPA and cariporide inhibit this recovery between 50–74% (Table 1), NHE-1 probably accounts for nearly two-thirds of pH_i recovery in NTS neurons. Furthermore, S1611 inhibits 26% of recovery, while 18% of neurons have their recovery inhibited by S1611, suggesting that ~20% of NTS neurons contain NHE-3, which is active in pH_i recovery from acidification. Thus, NHE-1 and -3 account for nearly all pH_i recovery from acid loads in NTS neurons, with other isoforms (e.g., NHE-5) playing, at most, a small part.

The picture is quite different in LC neurons. While recovery is entirely inhibited by Na-free solutions and unaffected by DIDS, as in neurons from the other two brainstem regions, amiloride has no effect on pH_i recovery in LC neurons (Fig. 5; Table 1). The only NHE inhibitor that has any effect on pH_i recovery is EIPA, and this results in, at most, a small inhibition at very high EIPA concentrations. Finally, only 2% of LC neurons show inhibition with S1611. These data suggest that LC neurons, unlike NTS and RTN neurons, have relatively low NHE activity. The presence of non-NHE-mediated recovery from acidification in LC neurons that is Na-dependent and DIDS-insensitive suggests the presence of HCO_3-dependent recovery, possibly NBCn1 (13). A strong HCO_3-dependence to this recovery is further supported by the fact that recovery from acidification is faster in the presence of CO_2/HCO_3 than in its absence in LC neurons (Fig. 9). Based on these findings, we propose that the majority of recovery of pH_i from acidification in LC neurons is mediated by NBCn1, although definitive proof for the presence of this transporter in LC neurons will require the use of RT-PCR or the use of specific antibodies for NBCn1.

Role of NHE-3 in central ventilatory control. Our studies suggest that NHE-3 is present in, at most, a few neurons from three different central chemosensitive regions, with the greatest presence being in NTS neurons. This would appear to be at odds with data suggesting that NHE-3 plays an important role in the control of breathing. In studies using organotypic cultures of VLM neurons, cariporide was applied to inhibit NHE-1 and no acidification or activation of neurons was observed (53, 58). We have observed a similar lack of effect of an NHE-1 inhibitor, amiloride, on steady-state pH_i in NTS neurons (41). These data are consistent with the lack of a stimulating effect of cariporide on phrenic nerve activity in the working heart brainstem preparation (57). In contrast to these effects of NHE-1 inhibitors, the NHE-3 inhibitors S1611 and S3226 evoked changes in the neuronal pH_i and firing rate similar to those experienced during hypercapnia (53, 58). Furthermore, an in vivo study was performed that suggested that the level of expression of NHE-3 mRNA in the brainstem was inversely correlated with ventilation, suggesting that NHE-3 plays a role in the determination of central respiratory drive in rabbits (54, 56). Expression levels of NHE-3 has also been shown to be altered in children that die of sudden infant death syndrome, compared with the expression level of children dying from non-sudden infant death syndrome-related causes (55). A brain-permeant inhibitor of NHE-3 increases respiration in adult rabbits (23). This latter study also found a few neurons within the brainstem that were immunoreactive for an NHE-3 antibody. Finally, infusion of an NHE-3 inhibitor into anesthetized rats resulted in increased ventilatory frequency (although neither tidal volume nor minute ventilation were increased) (40). This increase in respiratory frequency was accompanied by increased c-FOS staining in pre-Bötzinger complex and RTN neurons but not NTS neurons (40). Together, these data suggest that NHE-3 plays a role in central ventilatory control.

We do not believe that our findings are at odds with these findings. First, we find relatively few neurons that show putative NHE-3 activity. This accords with the findings of low levels of expression of NHE-3 mRNA in rat brainstem (24),

Table 1. *The %inhibition of mean pH_i recovery from NH_4Cl-induced acidification by various transport inhibitors*

Brainstem Area	DIDS/BDT	0 Na^+/NDT	AMIL/NHE	EIPA/NHE-1	CARIP/NHE-1	S1611/NHE-3
Retrotrapezoid nucleus	0	86	93	65	40	0 [5–10]*
Nucleus tractus solitarius	0	81	65	50	74	26 [18]*
Locus coeruleus	0	100	0	0–33	0	0 [2]*

Values are percentages. AMIL, amiloride; CARIP, cariporide; S1611, reasonably specific inhibitor for NHE-3; BDT, HCO_3-dependent transporters; NDT, Na-dependent transporters; NHE, Na^+/H^+ exchangers; NHE-1, Na^+/H^+ exchanger isoform 1; NHE-3, Na^+/H^+ exchanger isoform 3. *Number in brackets is %individual neurons whose recovery is inhibited by S1611.

relatively few brainstem neurons found to be immunohistochemically positive for NHE-3 (23), and reports that NHE-3 is functionally present in chemosensitive neurons from the VLM (53). Thus, widespread NHE-3 activity in the brainstem would not be expected. It is believed that central chemosensitivity arises from a distributed network (31). The evidence that specific inhibitors of NHE-3 in the VLM results in increased ventilation is not in conflict with our findings. Furthermore, NHE-3 likely also works on neurons from the pre-Bötzinger complex (40), which are believed to be involved in respiratory rhythm generation (16) and to be chemosensitive (48). NHE-3 may be expressed on glial cells as well, which have been shown to affect ventilatory control (15, 20). Kiwull-Schöne et al. (23) suggested that NHE-3 inhibitors may work by inhibiting NHE-3 in and altering the properties of other components of the complex respiratory network, and not simply by working on central chemosensitive neurons. Finally, inhibitors of NHE-3 seem in some cases to affect respiratory frequency more than tidal volume (40) and to cause only a fraction of the ventilatory increase caused by systemic hypercapnia (23). These latter findings are consistent with NHE-3 inhibitors affecting, at most, a few chemosensitive sites, with NHE-3 activity not being involved in chemoreception in neurons from other sites. This is consistent with a distributed chemosensitive network (31).

Response of pH_i to hypercapnia. Upon exposure to hypercapnia, the neurons from all three regions maintained a new, more acid, steady-state pH_i. Without additional experiments, we cannot differentiate whether this was due to a complete inhibition of the pH-regulating transporters in these neurons or to a new balance between acid loading and extruding mechanisms. We have previously shown that in NTS neurons a decrease of pH_o to 7.0 was sufficient to inhibit NHE (41) and that this transporter was more sensitive to inhibition by pH_o than the NHE in neurons from nonchemosensitive brainstem regions. However, it would be remarkable if hypercapnia fully inhibited the various NHEs in RTN and NTS neurons as well as the Na- and HCO_3-dependent transporter from LC neurons. Also, the relatively small intracellular acidification seen in response to 15% CO_2 implies that these neurons have a very high buffering power, which in fact, has been shown for NTS neurons (41). Nevertheless, our data confirm previous findings that a maintained acidification in response to hypercapnic acidosis is invariably seen in a variety of CO_2/H^+-sensitive cells.

Perspectives and Significance

Our data clearly indicate that pH-regulating transporters differ in neurons from different chemosensitive regions, with multiple NHE isoforms mediating recovery from acidification in RTN and NTS neurons but a Na- and HCO_3-dependent transporter predominating in LC neurons (Table 1). These latter findings are the first demonstration of functional HCO_3-dependent transport in neurons from central chemosensitive brainstem regions, although such transporters have been demonstrated in glomus cells of the carotid bodies (10), the peripheral chemoreceptors. It is noteworthy that despite the fact that the neurons from these different chemosensitive regions contain various pH-regulating transporters, no pH_i recovery from acidification is observed during hypercapnic acidosis (Fig. 2). That hypercapnic acidosis results in a lack of pH_i recovery in the neurons from all of these brainstem regions suggests that changes of pH are an important part of the signaling mechanism in chemosensitive neurons (17, 38).

A major question in the field of respiratory control is why there are so many central chemosensitive sites (30, 31). It has been suggested that these sites may have arisen in a hierarchical fashion (28) as organisms passed through critical changes during phylogeny, such as emerging from an aqueous environment to become air breathing, the development of the ability to maintain a high, constant body temperature, and the development of sleep. If respiratory control did indeed develop in a polyphyletic fashion, then it might be expected that neurons from different chemosensitive regions may have developed different cellular mechanisms of chemosensitivity, including differences in the regulation of pH_i. Thus, our finding of differences in the pH-regulating transporters in neurons from different chemosensitive regions may at least be consistent with a polyphyletic origin of multiple central chemoreceptive sites.

Finally, it is clear that the maintenance of acidification during hypercapnic acidosis requires inhibition of different pH-regulating transporters in neurons from different chemosensitive regions. If highly specific inhibitors could be found for each of these transporters, then it might be possible to use these inhibitors focally to study the role of each chemosensitive region in ventilatory control. This would allow us to start to address the question of why there are so many central chemosensitive regions and what the role of each region is in respiratory control.

ACKNOWLEDGMENTS

We thank Phyllis Douglas for her technical support. We also acknowledge Anne Griffith and the Miami Valley School for support of A. E. Kersh.

Cariporide and S1611 were generous gifts from Sanofi-Aventis Pharmaceutical.

GRANTS

This work was supported by National Heart, Lung, and Blood Institute Grants R01-HL-56683 (to R. W. Putnam and J. B. Dean), F32-HL-080877 (to L. K. Hartzler), and T35-HL-07805 (to J. Chua and B. Belcastro Hubbell), as well as by an American Heart Association (Ohio Valley Affiliate) Summer Undergraduate Research Fellowship (to A. Kalra).

REFERENCES

1. **Andrzejewski M, Mückenhoff K, Scheid P, Ballantyne D.** Synchronized rhythms in chemosensitive neurons of the locus coeruleus in the absence of chemical synaptic transmission. *Respir Physiol* 129: 123–140, 2001.
2. **Attaphitaya S, Park κ, Melvin JE.** Molecular cloning and functional expression of rat Na^+/H^+ exchanger (NHE5) highly expressed in brain. *J Biol Chem* 274: 4383–4388, 1999.
3. **Bachmann O, Riederer B, Rossmann H, Groos S, Schultheis PJ, Shull GE, Gregor M, Manns MP, Seidler U.** The Na^+/H^+ exchanger isoform 2 is the predominant NHE isoform in murine colonic crypts and its lack causes NHE3 upregulation. *Am J Physiol Gastrointest Liver Physiol* 287: G125–G133, 2004.
4. **Bevensee MO, Cummins TR, Haddad GG, Boron WF, Boyarsky G.** pH regulation in single CA1 neurones acutely isolated from the hippocampi of immature and mature rats. *J Physiol* 494: 315–328, 1996.
5. **Bevensee MO, Schmitt BM, Choi I, Romero MF, Boron WF.** An electrogenic Na/HCO_3 co-transporter (NBC) with a novel C terminus, cloned from rat brain. *Am J Physiol Cell Physiol* 278: C1200–C1211, 2000.
6. **Bevensee MO, Schwiening CJ, Boron WF.** Use of BCECF and propidium iodide to assess membrane integrity of acutely isolated CA1 neurons from rat hippocampus. *J Neurosci Meth* 58: 61–75, 1995.

7. **Bookstein C, Musch MW, DePaoli A, Xie Y, Rabenau K, Villereal M, Rao MC, Chang EB.** Characterization of the rat Na^+/H^+ exchanger isoform NHE4 and localization in rat hippocampus. *Am J Physiol Cell Physiol* 271: C1629–C1638, 1996.
8. **Boron WF, De Weer P.** Intracellular pH transients in squid giant axons caused by CO_2, NH_3, and metabolic inhibitors. *J Gen Physiol* 67: 91–112, 1976.
9. **Bouyer P, Bradley SR, Zhao J, Wang W, Richerson GB, Boron WF.** Effect of extracellular acid-base disturbances on the intracellular pH of neurones cultured from rat medullary raphé or hippocampus. *J Physiol* 559: 85–101, 2004.
10. **Buckler KJ, Vaughan-Jones RD, Peers C, Nye PCG.** Intracellular pH and its regulation in isolated type 1 carotid body cells of the neonatal rat. *J Physiol* 436: 107–129, 1991.
11. **Chambrey R, Achard JM, Warnock DG.** Heterologous expression of rat NHE4: a highly amiloride-resistant Na^+/H^+ exchanger isoform. *Am J Physiol Cell Physiol* 272: C90–C98, 1997.
12. **Chesler M.** The regulation and modulation of pH in the brain. *Physiol Rev* 83: 1183–1221, 2003.
13. **Choi I, Aalkjaer C, Boulpaep EL, Boron WF.** An electroneutral sodium/bicarbonate cotransporter NBCn1 and associated sodium channel. *Nature* 405: 571–575, 2000.
14. **Cooper DS, Sacena NC, Yang HS, Lee HJ, Moring AG, Lee A, Choi I.** Molecular and functional characterization of the electroneutral Na/HCO_3 cotransporter NBCn1 in rat hippocampal neurons. *J Biol Chem* 280: 17823–17830, 2005.
15. **Erlichman JS, Li A, Nattie EE.** Ventilatory effects of glial dysfunction in a rat brain stem chemoreceptor region. *J Appl Physiol* 85: 1599–1604, 1998.
16. **Feldman JR, Mitchell GS, Nattie EE.** Breathing: rhythmicity, plasticity, chemosensitivity Ann Rev Neurosci 26: 239–266, 2003.
17. **Filosa JA, Dean JB, Putnam RW.** Role of intracellular and extracellular pH in the chemosensitive response of rat locus coeruleus neurones. *J Physiol* 541: 493–509, 2002.
18. **Gaillard S, Dupont J.** Ionic control of intracellular pH in rat cerebellar Purkinje cells maintained in culture. *J Physiol* 425: 71–83, 1990.
19. **Goldstein JI, Mok JM, Simon CM, Leiter JC.** Intracellular pH regulation in neurons from chemosensitive and nonchemosensitive regions of *Helix aspersa*. *Am J Physiol Regul Integr Comp Physiol* 279: R414–R423, 2000.
20. **Holleran J, Babbie M, Erlichman JS.** Ventilatory effects of impaired glial function in a brain stem chemoreceptor region in the conscious rat. *J Appl Physiol* 90: 1539–1547, 2001.
21. **Kersh AE, Kalra A, Ritucci NA, Dean JB, Putnam RW.** Intracellular pH (pH_i) regulation in neurons from a chemosensitive region of the retrotrapezoid nucleus (RTN) of neonatal rats (Abstract). *FASEB J* 19: A647, 2005.
22. **Kiwull-Schöne H, Wiemann M, Frede S, Bingmann D, Kiwull P.** Tentative role of the Na^+/H^+ exchanger type 3 in central chemosensitivity of respiration. *Adv Exp Med Biol* 536: 415–421, 2003.
23. **Kiwull-Schöne H, Wiemann M, Frede S, Bingmann D, Wirth KJ, Heinelt U, Lang HJ, Kiwull P.** A novel inhibitor of the Na^+/H^+ exchanger type 3 activates the central respiratory CO_2 response and lowers the apneic threshold. *Am J Respir Crit Care Med* 164: 1303–1311, 2001.
24. **Ma E, Haddad GG.** Expression and localization of Na^+/H^+ exchangers in rat central nervous system. *Neuroscience* 79: 591–603, 1997.
25. **Masereel B, Pochet L, Laeckmann D.** An overview of inhibitors of Na^+/H^+ exchanger. *Eur J Med Chem* 38: 547–554, 2003.
26. **Mulkey DK, Stornetta RL, Weston MC, Simmons JR, Parker A, Bayliss DA, Guyenet PG.** Respiratory control by ventral surface chemoreceptor neurons in rats. *Nat Neurosci* 7: 1360–1369, 2004.
27. **Nakamura N, Tanaka S, Teko Y, Mitsui K, Kanazawa H.** Four Na^+/H^+ exchanger isoforms are distributed to Golgi and post-Golgi compartments and are involved in organelle pH regulation. *J Biol Chem* 280: 1561–1572, 2005.
28. **Nattie EE.** Central chemosensitivity, sleep, wakefulness. *Respir Physiol* 129: 257–268, 2001.
29. **Nattie EE, Li A.** CO_2 dialysis in nucleus tractus solitarius region of rat increases ventilation in sleep and wakefulness. *J Appl Physiol* 92: 2119–2130, 2002.
30. **Nattie EE, Li A.** Central chemoreception 2005: a brief review. *Auton Neurosci* 126–127: 332–338, 2006.
31. **Nattie EE, Li A.** Central chemoreception is a complex system function that involves multiple brainstem sites. *J Appl Physiol* 106: 1464–1466, 2009.
32. **Nottingham S, Leiter JC, Wages P, Buhay S, Erlichman JS.** Developmental changes in intracellular pH regulation in medullary neurons of the rat. *Am J Physiol Regul Integr Comp Physiol* 281: R1940–R1951, 2001.
33. **Orlowski J, Grinstein S.** Diversity of the mammalian sodium/proton exchanger SLC9 gene family. *Pflügers Arch* 447: 549–565, 2004.
34. **Ou-yang Y, Mellergård P, Siesjö BK.** Regulation of intracellular pH in single rat cortical neurons in vitro: a microspectrofluorometric study. *J Cereb Blood Flow Metab* 13: 827–840, 1993.
35. **Pizzonia JH, Biemesderfer D, Abu-Alfa AK, Wu MS, Exner M, Isenring P, Igarashi P, Aronson PS.** Immunochemical characterization of Na^+/H^+ exchanger isoform NHE4. *Am J Physiol Renal Physiol* 275: F510–F517, 1998.
36. **Pocock G, Richards CD.** Hydrogen ion regulation in rat cerebellar granule cells studied by single-cell fluorescence microscopy. *Eur J Neurosci* 4: 136–143, 1992.
37. **Putnam RW.** Intracellular pH regulation of neurons in chemosensitive and nonchemosensitive areas of brain slices. *Respir Physiol* 129: 37–56, 2001.
38. **Putnam RW, Filosa JA, Ritucci NA.** Cellular mechanisms involved in CO_2 and acid signaling in chemosensitive neurons. *Am J Physiol Cell Physiol* 287: C1493–C1526, 2004.
39. **Raley-Susman KM, Sapolsky RM, Kopito RR.** Cl^-/HCO_3^- exchange function differs in adult and fetal rat hippocampal neurons. *Brain Res* 614: 308–314, 1993.
40. **Ribas-Salgueiro JL, Matarredona ER, Sarmiento M, Ribas J, Pásaro R.** Respiratory response to systemic inhibition of the Na^+/H^+ exchanger type 3 in intact rats. *Respir Physiol Neurobiol* 165: 254–260, 2009.
41. **Ritucci NA, Chambers-Kersh L, Dean JB, Putnam RW.** Intracellular pH regulation in neurons from chemosensitive and nonchemosensitive areas of the medulla. *Am J Physiol Regul Integr Comp Physiol* 275: R1152–R1163, 1998.
42. **Ritucci NA, Dean JB, Putnam RW.** Intracellular pH response to hypercapnia in neurons from chemosensitive areas of the medulla. *Am J Physiol Regul Integr Comp Physiol* 273: R433–R441, 1997.
43. **Ritucci NA, Erlichman JS, Dean JB, Putnam RW.** A fluorescence technique to measure intracellular pH of single neurons in brainstem slices. *J Neurosci Meth* 68: 149–163, 1996.
44. **Ritucci NA, Erlichman JS, Leiter JC, Putnam RW.** The response of membrane potential (V_m) and intracellular pH (pH_i) to hypercapnia in neurons and astrocytes from rat retrotrapezoid nucleus (RTN). *Am J Physiol Regul Integr Comp Physiol* 289: R851–R861, 2005.
45. **Romero MF, Fulton CM, Boron WF.** The SLC4 family of HCO_3^- transporters. *Pflügers Arch* 447: 495–509, 2004.
46. **Schwark JR, Jansen HW, Lang HJ, Krick W, Burckhardt G, Hropot M.** S3226, a novel inhibitor of Na^+/H^+ exchanger subtype 3 in various cell types. *Pflügers Arch* 436: 797–800, 1998.
47. **Schwiening CJ, Boron WF.** Regulation of intracellular pH in pyramidal neurons from the rat hippocampus by Na^+-dependent Cl^--HCO_3^- exchange. *J Physiol* 475: 59–67, 1994.
48. **Solomon I, Edelman N, O'Neal M.** CO_2/H^+ chemoreception in the cat pre-Bötzinger complex in vivo. *J Appl Physiol* 88: 1996–2007, 2000.
49. **Thomas JA, Buchsbaum RN, Zimniak A, Racker E.** Intracellular pH measurements in Ehrlich ascites tumor cells utilizing spectroscopic probes generated in situ. *Biochemistry* 81: 2210–2218, 1979.
50. **Tolkovsky AM, Richards CD.** Na^+/H^+ exchange is the major mechanism of pH regulation in cultured sympathetic neurons: measurements in single cell bodies and neurites using a fluorescent pH indicator. *Neuroscience* 22: 1093–1102, 1987.
51. **Wang W, Bradley SR, Richerson GB.** Quantification of the response of rat medullary raphé neurones to independent changes in pH_o and P_{CO_2}. *J Physiol* 540: 951–970, 2002.
52. **Wang Z, Orlowski J, Shull GE.** Primary structure and functional expression of a novel gastrointestinal isoform of the rat Na/H exchanger. *J Biol Chem* 268: 11925–11928, 1993.
53. **Wiemann M, Bingmann D.** Ventrolateral neurons of medullar organotypic cultures: intracellular pH regulation and bioelectric activity. *Respir Physiol* 129: 57–70, 2001.

54. **Wiemann M, Frede S, Bingmann D, Kiwull P, Kiwull-Schöne H.** Sodium/proton exchanger 3 in the medulla oblongata and set point of breathing control. *Am J Respir Crit Care Med* 172: 244–249, 2005.
55. **Wiemann M, Frede S, Tschentscher F, Kiwull-Schöne H, Kiwull P, Bingmann D, Brinkmann B, Bajanowski T.** NHE3 in the human brainstem: implication for the pathogenesis of the sudden infant death syndrome (SIDS)? *Adv Exp Med Biol* 605: 508–513, 2008.
56. **Wiemann M, Kiwull-Schöne H, Frede S, Bingmann D, Kiwull P.** Brainstem NHE-3 expression and control of breathing. *Adv Exp Med Biol* 551: 39–44, 2004.
57. **Wiemann M, Piechatzek L, Göpelt K, Kiwull-Schöne H, Kiwull P, Bingmann D.** The NHE3 inhibitor AVE1599 stimulates phrenic nerve activity in the rat. *J Physiol Pharmacol* 59: 27–36, 2008.
58. **Wiemann M, Schwark JR, Bonnet U, Jansen HW, Grinstein S, Baker RE, Lang HJ, Wirth KK, Bingmann D.** Selective inhibition of the Na^+/H^+ exchanger type 3 activates CO_2/H^+-sensitive medullary neurones. *Pflügers Arch* 438: 255–262, 1999.
59. **Xue J, Douglas RW, Zhou D, Lim JY, Boron WF, Haddad GG.** Expression of Na^+/H^+ exchanger isoform 1 null mutant mouse brain. *Neuroscience* 122: 37–46, 2003.